

Open Minds

Internacional Journal

ISSN 2675-5157

vol. 2, n.9, 2026

●●● ARTICLE 1

Acceptance date: 17/04/2026

DNA CONDENSATION THROUGH FUNCTIONALIZATION OF STYRENE-CO-MALEIC ANHYDRIDE COPOLYMER (SMA) WITH TALLOW AMINE

Laura Margarita Salcedo Flores

Departamento de Ciencias Biomédicas, Centro Universitario de Tonalá, Universidad de Guadalajara, Tonalá, México.

Roberto Carlos Cortes Cortes

Departamento de Ciencias Básica Aplicadas, Centro Universitario de Tonalá, Universidad de Guadalajara, Tonalá, México.

Víctor Hugo Antolín Cerón

Departamento de Ciencias Básica Aplicadas, Centro Universitario de Tonalá, Universidad de Guadalajara, Tonalá, México.

José de Jesús Cabrera Chavarriab

Departamento de Ciencias Básica Aplicadas, Centro Universitario de Tonalá, Universidad de Guadalajara, Tonalá, México.

Julieta Carrasco García

Departamento de Ciencias Básica Aplicadas, Centro Universitario de Tonalá, Universidad de Guadalajara, Tonalá, México.



All content published in this journal is licensed under the Creative Commons Attribution 4.0 International License (CC BY 4.0).

nities for the treatment of hereditary disorders such as cancer and congenital diseases, as well as other conditions including HIV infection, diabetes, Parkinson's disease, and Alzheimer's disease. A key component of gene therapy is the use of vectors, molecular vehicles capable of delivering genetic material into host cells, enabling the introduction of functional DNA sequences.

Vector-based systems are also widely used for the extraction and stabilization of membrane-associated proteins. In particular, amphiphilic polymers can encapsulate fragments of cellular membranes to form nanodiscs, which preserve the native environment of membrane proteins. These nanostructures enable the study of protein function and structure and are increasingly used in drug discovery, biomarker identification, vaccine development, antibody production, and structural biology.

Among amphiphilic polymers, poly(styrene-co-maleic anhydride) (SMA) copolymers have attracted considerable attention due to their ability to solubilize lipid membranes and form self-assembled nanostructures. [klosgen 2009, Knwoles 2009] Their amphiphilic architecture, consisting of hydrophobic aromatic styrene units and chemically reactive maleic anhydride groups, allows further functional modification. SMA has been successfully employed for membrane solubilization, protein encapsulation, and the formation of polymer-lipid nanodiscs with high structural adaptability. [Jamshad 2011, Dorr 2014, Oluwole 2017] However, after hydrolysis of the maleic anhydride groups, SMA typically exhibits a net negative charge, which limits its direct interaction with negatively charged biomolecules such as DNA.

Cationic polymers are widely used as condensing agents for nucleic acids and proteins due to their ability to interact electrostatically with negatively charged biomolecules. Several studies have reported SMA-based systems modified with cationic polymers such as low-molecular-weight polyethylenimine, dendrimers, or chitosan, which promote DNA condensation through electrostatic interactions. [Godbey 1999, Lavertu 2006, Mintzer 2009] [Duan 2012]. Despite their effectiveness, these systems may present limitations including cytotoxicity, reduced colloidal stability, or limited control over self-assembly, highlighting the need for alternative amphiphilic materials with tunable physicochemical properties. [Winel 1977, Maeda 2001, Zovko 2005] .

Tallow amine, a derivative of animal fat composed of a primary amine attached to a hydrocarbon chain containing approximately 12–16 carbon atoms, represents an attractive candidate for polymer functionalization. These compounds are commonly used as precursors for cationic surfactants and are widely applied in agrochemicals, asphalt emulsions, flotation processes in mining, dispersants, and antistatic agents.

The chemical modification of SMA with long-chain amines such as tallow amine introduces protonable cationic groups together with hydrophobic aliphatic segments, generating a highly amphiphilic copolymer capable of combining electrostatic interactions with hydrophobic stabilization. This modification may promote DNA condensation through partial charge neutralization while simultaneously facilitating the formation of compact and stable structures in aqueous media. Furthermore, hydrophobic domains may enhance interactions with globular proteins, expanding the

intracellular components. Proteins and other cellular contaminants were subsequently removed through a precipitation step, allowing the genomic DNA to remain in solution. The DNA was then precipitated using alcohol and collected by centrifugation. After washing to eliminate residual salts and impurities, the purified genomic DNA was rehydrated in an appropriate buffer solution. The resulting DNA was suitable for downstream applications such as molecular analysis and biochemical characterization.

Critical micelle concentration (CAC)

The critical aggregation concentration (CAC) was determined using complementary physicochemical techniques. Surface tension measurements were performed using the Du Noüy ring method. Electrical conductivity was measured with a Thermo Scientific Orion Star A212 conductivity meter, while electrical resistivity was recorded using a digital multimeter. For each method, the CAC was obtained by plotting the measured property as a function of polymer concentration and identifying the breakpoint corresponding to the transition between the pre-micellar and micellar regimes.

Preparation of polymer-DNA complexes

All polymers DNA and protein complexes were freshly prepared before use by adding different concentration of polymer solution into equal volumes, to obtain the desired polymer nitrogen to DNA. Followed by vortexing for 30 seconds and incubating at room temperature for 30 minutes.

Optical Microscopy

Samples were placed on a viewing slide (covered with a cover slip in the case of the largest magnification) and observed with an optical microscope (Amscope). A 20×, 40× and 100× objective lens was used to record sample microstructure.

Dispersion Light Scattering (DLS)

Dynamic light scattering (DLS) measurements were performed using a Malvern Zetasizer Nano ZS90 instrument. The samples were placed in 10 mL quartz cuvettes prior to analysis.

Theoretical calculations

Molecular interaction field (MIF) maps, also known as contact density fields (CDFs), as well as electrostatic potential maps, were generated for representative fragments of DNA and the SMA copolymer using the Spartan program. The calculations were performed within the framework of density functional theory (DFT) employing the B3LYP functional and the cc-pVTZ basis set.

Results

Dispersion light scattering (DLS)

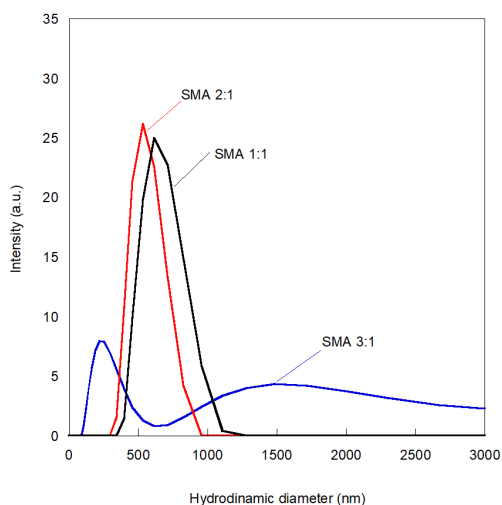


Figure 1. Distribution of hydrodynamic diameter of SMA family's copolymer in water

The hydrodynamic diameter of the three surfactants used for polyurethane (PU) emulsification is shown in the figure. Copolymers with lower styrene content exhibit a single and relatively narrow size distribution with low polydispersity (See table 1). This behavior can be attributed to their higher hydrophilicity, which favors greater solubility in water and promotes the presence of extended polymer chains in solutions. Under these conditions, the copolymer remains predominantly dispersed as individual chains or small aggregates. In contrast, as the styrene content in the surfactant increases, two distinct size populations are observed in the DLS measurements. This behavior is associated with the increased hydrophobicity of the copolymer, which reduces its affinity for the aqueous phase and promotes intermolecular hydrophobic interactions that produces smaller particles

and also, the polymer chains tend to self-associate, forming larger aggregates or micelle-like structures. The larger particle population exhibits lower scattering intensity, suggesting the formation of heterogeneous assemblies and a broader distribution of aggregate sizes [Craig 2019]. This behavior is characteristic of amphiphilic copolymers in aqueous media, where a balance between hydrophobic interactions among styrene units and the hydrophilic character of the maleic acid groups governs the self-assembly process. Previous studies have employed dynamic light scattering (DLS) to characterize particle size distributions in polymer systems based on SMA copolymers, including the formation of polymer–lipid nanostructures and the control of nanoparticle size using SMA variants and lipid mixtures. These reports describe aggregation and size distribution trends similar to those observed in the present system [Craig 2016; Harding 2019; Lee 2022].

Critical micelle concentration (CMC)

Figure 2 presents the plots used to identify the concentration at which SMA aggregates or micelle-like structures form in aqueous solution, using different experimental techniques.

Figure 2a shows the variation in electrical resistivity as a function of SMA concentration. A sharp decrease in resistivity is observed at very low surfactant concentrations, followed by stabilization near 1 wt% SMA. This behavior suggests that the resistivity of the medium decreases due to the high polarity of the maleic anhydride units, which promote ionic conduction pathways in water. Additionally, the increasing connectivity between polymer chains at higher

concentrations may facilitate charge transport through the solution. [Lee 2004, Florjanczyk 2000, Vink 1989].

An opposite trend is observed when electrical conductivity is measured using a conductivity meter (Figure 2b). In this case, conductivity increases with SMA concentration, which can be attributed to the high density of carboxylic groups generated by hydrolysis of the maleic anhydride units. When SMA is dispersed in water, the anhydride ring undergoes hydrolytic opening, producing carboxylate groups (COO^-) and protons (H^+), which enhance ionic mobility and increase the overall ionic transport in the aqueous phase. This phenomenon is characteristic of polyelectrolyte behavior and has been reported previously for hydrolyzed SMA systems in aqueous environments.

Finally, Figure 2c shows the surface tension measurements obtained using the Du Noüy ring method. A change in the linearity of the curve is observed at approximately 1.5 wt% SMA, which may indicate the onset of polymer aggregation in solution. However, the SMA solutions display a gradual increase in surface tension with increasing concentration, rather than the sharp inflection point typically associated with the critical micelle concentration (CMC) of conventional low-molecular-weight surfactants. [Noskov 2011. Loglio, (2001)] This behavior suggests a progressive adsorption of the amphiphilic copolymer at the air–water interface, rather than the formation of well-defined micelles. Such behavior is common for amphiphilic copolymers with relatively large molecular chains, where the interfacial adsorption process competes with bulk self-assembly processes. In these systems, the formation of polymeric aggregates, large polymeric micelles, or hydrophobic clusters

may occur in solution, and these structures do not readily migrate to the air–water interface. Consequently, the observed surface tension behavior may be associated with interfacial structuring effects or changes in the composition of the medium, reflecting the aggregation behavior typical of amphiphilic copolymers in aqueous systems. [Wright (2015). Scheidelaar,(2016)]

Infrared spectroscopy

The infrared spectra were normalized in the range from 0 to 1 in order to allow proper comparison of signal intensities. Figure 3a shows the full FTIR spectrum of the SMA 2:1 copolymer (green line) in aqueous solution used as reference. The spectrum exhibits the characteristic vibrational bands of the copolymer. At lower wavenumbers, several typical bands can be observed, including the band at $700\text{--}760\text{ cm}^{-1}$, associated with out-of-plane C–H bending of the aromatic ring. Additional bands are observed in the $1100\text{--}1250\text{ cm}^{-1}$ region, which can be attributed to C–O and C–O–C stretching vibrations associated with the hydrolyzed maleic anhydride groups and possible ether or ester linkages formed after modification. The band near $1600\text{--}1650\text{ cm}^{-1}$ corresponds to aromatic and conjugated C=C stretching vibrations of the styrene units. A weak shoulder around $1715\text{--}1730\text{ cm}^{-1}$ can be assigned to C=O stretching vibrations of carboxylic acid groups generated after hydrolysis of the maleic anhydride units. In addition, a weak band around $1780\text{--}1850\text{ cm}^{-1}$ may be associated with residual maleic anhydride carbonyl groups, although their intensity is typically low in hydrolyzed systems. At higher wavenumbers, bands at 2920 cm^{-1} and 2850 cm^{-1} correspond to asymmetric and symmetric stretching vibra-

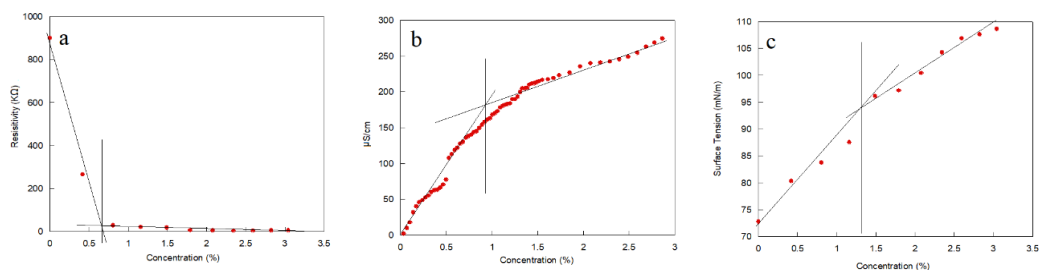


Figure 2. Critical aggregation concentration obtained of SMA 2:1 by: a) resistivity, b) conductivity and c) surface tension

Sample	CAC (% wt/wt)			Hydrodynamic diameter (nm)	Polydispersity index (DPI)
	Surface tension	Resistivity	conductivity		
SMA 1:1	1.32	0.95	1.52	633	0.19
SMA 2:1	1.48	0.98	1.17	550	0.18
SMA 3:1	1.50	1.22	2.3	225,1441	0.83

Table 1. Critical aggregation concentration (CAC) and hydrodynamic radius (Rh) of SMA copolymers in aqueous solution.

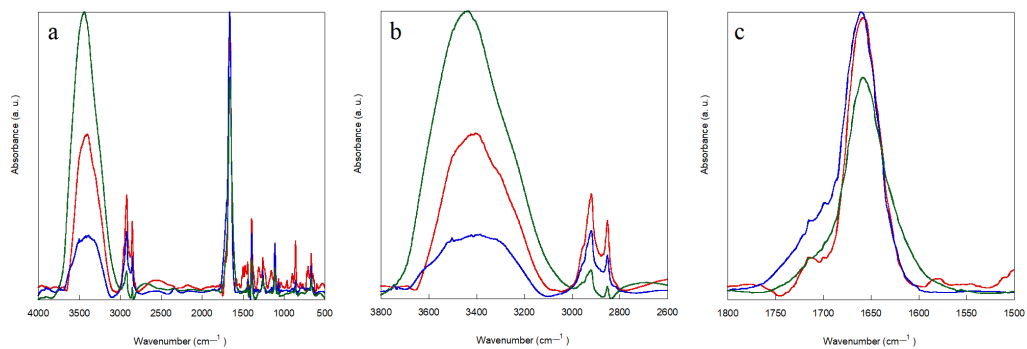


Figure 3 infrared spectra of SMA With DNA: a) Whole spectra, b) amine-hydroxyl zone and c) carbonyl zone

tions of aliphatic $-\text{CH}_2$ and $-\text{CH}_3$ groups, which are consistent with the presence of the long hydrocarbon chain of the tallow amine modifier. A broad band centered near $3300\text{--}3400\text{ cm}^{-1}$ is attributed to O–H stretching vibrations, mainly associated with water molecules and hydrogen-bonded hydroxyl groups present in the aqueous system. All these bands are reported by several authors that work with modified and hydrolyzed SMA [Knowles 2009, Dörr 2014, Oluwole 2017, Harding 2019]

The spectra shown in red and blue in figure 3b and 3c correspond to SMA 2:1 and SMA 3:1 in the presence of DNA, respectively. In these spectra, additional spectral contributions associated with the interaction between DNA and the SMA copolymer can be observed. One of the most noticeable differences is the appearance of bands in the region between 1500 and 1700 cm^{-1} , which are mainly associated with in-plane vibrational modes of nucleobases, including overlapping C=O, C=C, and C=N stretching vibrations of heterocyclic bases present in DNA. As shown in Figure 1c, small shoulder peaks appear around 1580 cm^{-1} and $1700\text{--}1710\text{ cm}^{-1}$, together with an increase in the intensity of aromatic and heterocyclic double-bond vibrations. These bands are consistent with the spectral fingerprints of nucleobases reported in FTIR studies of DNA. [Muntean 2014, Custovic 2022]

Another noticeable change is the decrease in intensity of the broad O–H stretching band, suggesting the involvement of hydrogen bonding interactions between the polymer matrix and DNA. This effect appears to be more pronounced in the SMA 2:1 system, indicating stronger interaction with DNA compared to SMA 3:1. The lower

spectral contribution observed for SMA 3:1 may be related to its higher styrene content and increased hydrophobicity, which reduces its affinity toward the hydrophilic DNA backbone.

Overall, the FTIR results suggest that the SMA 2:1 copolymer exhibits stronger interactions with DNA than the more hydrophobic SMA 3:1 variant.

Because DNA condensation occurs in an aqueous medium, spectral subtraction was performed in order to isolate the spectral contribution of the encapsulated DNA from the signals of water and the SMA copolymer. The SMA 2:1 copolymer was selected for this analysis because visual inspection of the spectra suggested a stronger interaction with DNA compared to the other formulations.

Figure 4a shows the FTIR spectrum of the SMA copolymer in aqueous solution. The supernatant obtained after mixing the copolymer with DNA in water was subsequently analyzed (inset Figure 4b). After applying spectral subtraction to remove the contributions of water and the polymer matrix, the resulting spectrum revealed several characteristic vibrational bands commonly reported for hydrated DNA. The spectrum exhibits most of the infrared features previously described for nucleic acids in aqueous environments (Mao et al., 1994; Banyay et al., 2003; Wood et al., 2016). A broad band centered at approximately 3390 cm^{-1} is observed and can be attributed to overlapping O–H stretching vibrations from hydrogen-bonded water molecules together with N–H stretching modes from nucleobases. This broad absorption is typical for hydrated nucleic acids where extensive hydrogen bonding occurs between the

phosphate backbone, nucleobases, and surrounding water molecules.

In the fingerprint region, several characteristic DNA bands are detected. The band located near 1085 cm^{-1} corresponds to the symmetric stretching vibration of the phosphate group (PO_2^-) in the DNA backbone, while the signal around 1230 cm^{-1} is assigned to the asymmetric stretching vibration of PO_2^- groups. These bands are widely recognized as diagnostic markers of nucleic acid structures and are commonly used to monitor DNA interactions with polymers and other biomolecules (Banyay et al., 2003; Wood et al 2016). Additionally, a band near 970 cm^{-1} can be associated with backbone vibrations of the deoxyribose–phosphate framework, which are sensitive to conformational changes in DNA.

Within the spectral region highlighted in the inset of Figure 4, additional signals appear between 1600 and 1750 cm^{-1} , corresponding mainly to in-plane stretching and bending vibrations of nucleobases. The band near 1603 cm^{-1} can be attributed to C=N stretching vibrations associated with guanine, while the signal around 1643 cm^{-1} is related to C2=O stretching vibrations of cytosine. Furthermore, the band observed at approximately 1683 cm^{-1} corresponds to C6=O stretching of guanine and C4=O vibrations of thymine, which are commonly reported in FTIR studies of nucleic acid structure and intermolecular interactions (Mao et al., 1994; Banyay et al., 2003).

Overall, the presence of these characteristic phosphate and nucleobase vibrations confirms the presence of DNA within the polymeric environment and supports the formation of polymer–DNA complexes in aqueous solution. The observation of these bands after spectral subtraction suggests

that the SMA copolymer is capable of interacting with and stabilizing DNA structures through a combination of electrostatic interactions and hydrogen bonding.

Optical microscopy

Figure 5 shows optical microscopy images in which particles with an average diameter of $19 \pm 5\text{ }\mu\text{m}$ can be observed. These aggregates correspond to the SMA 2:1 sample in the presence of DNA, where the formed particles result from flocculation induced by polymer–DNA complexes. This phenomenon is mainly driven by the negative charge of DNA originating from the phosphate groups, which interact with the tallow amine functionalities of the modified SMA, generating strong electrostatic interactions commonly referred to as bridging interactions. Furthermore, SMA functionalized with tallow amine contains multiple interaction sites, allowing a single polymer chain to bind simultaneously to several DNA molecules. As a consequence, bridging aggregation occurs, leading to the formation of micrometer-sized aggregates with diameters close to $20\text{ }\mu\text{m}$. Similar behaviors have been reported for other cationic polymers capable of inducing DNA condensation, including polyethyleneimine (PEI), chitosan, and polylysine [Bloomfield, (1996). DeRouchey, (2010). Zinchenko, (2005).]. Comparable structures were not observed for the SMA 3:1 system, which is attributed to its weaker interaction with DNA, likely resulting from its higher styrene content and increased hydrophobicity, which reduce its effective electrostatic interaction with the polyanionic DNA backbone. Consistent with these observations, the increase in particle size detected by dynamic light scattering (DLS) upon addition of DNA suggests

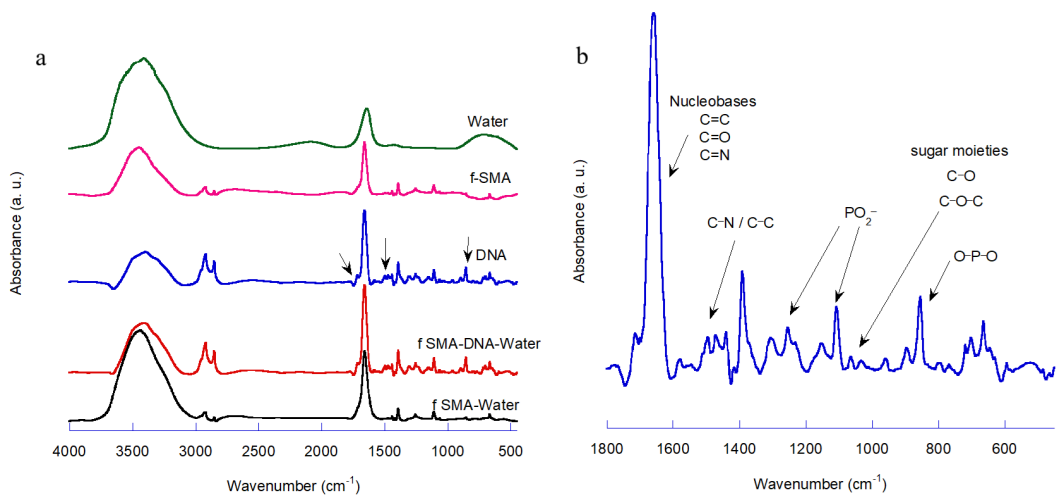


Figure 4. Infrared spectra of: a) SMA-water, b) SMA-DNA-water, c) subtracted spectra of DNA, d) SMA and e) water

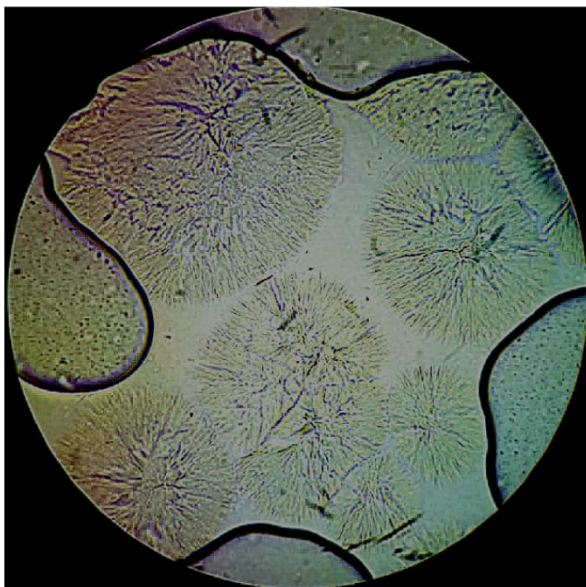


Figure 5. Optical microscopy image form SMA-DNA

a transition from amphiphilic SMA aggregates to larger polyelectrolyte complexes. These processes ultimately lead to the formation of micrometer-sized flocculated assemblies or polymer-rich coacervate-like structures, stabilized by hydrophobic domains derived from styrene units and tallow amine segments. [Spruijt, (2010).]

Figure 6 illustrates the different behaviors of DNA and egg albumin when exposed to the SMA copolymer. In Figure 4a, the tubes containing DNA are shown. It can be observed that DNA fragments become encapsulated within dispersed particles that, after approximately 24 h, tend to flocculate and accumulate at the upper part of the test tube, forming a visible supernatant enriched with DNA-containing aggregates. In contrast, the second tube in Figure 4a contains only SMA dispersed in water, which appears as a slightly whitish and homogeneous solution, indicating that the polymer remains dispersed in the aqueous medium in the absence of biomolecules.

Figure 6b presents the samples containing egg albumin. The sample labeled 0 corresponds to egg albumin dispersed in water, where a turbid suspension can be observed due to the presence of dispersed protein molecules. In contrast, when different proportions of SMA are added, the protein becomes trapped by the polymer and precipitates, leaving the aqueous phase noticeably clarified. This behavior suggests the formation of insoluble protein–polymer aggregates resulting from strong interactions between the albumin molecules and the amphiphilic SMA copolymer.

The observation that DNA flocculates whereas egg albumin precipitates can be explained by different physicochemical interaction mechanisms. Protein precipitation

commonly occurs through charge neutralization combined with hydrophobic interactions, which reduce electrostatic repulsion between protein molecules and promote intermolecular association and aggregation. Egg albumin contains internal hydrophobic domains that can interact with the aromatic styrene units and the hydrophobic chains derived from the tallow amine groups of the modified SMA. Such interactions may induce partial exposure of hydrophobic regions of the protein, leading to enhanced protein–protein interactions and the formation of large aggregates that eventually precipitate from solution. This phenomenon is often associated with protein–polymer complex aggregation or coacervation, which may lead to partial protein denaturation due to conformational rearrangements of the protein structure (Arakawa & Timasheff, 1985; Baldwin, 1996; Schmitt & Turgeon, 2011).

Consequently, the observed behavior in the albumin system corresponds mainly to protein precipitation rather than true encapsulation or controlled condensation. Although such conformational changes may limit applications in biomedical fields such as gene therapy, these protein–polymer aggregates may still be useful for industrial applications, including the development of hydrogels, adsorbent materials, food structuring systems, biomaterials, and polymer compatibilizers.

In contrast, the interaction between SMA and DNA appears to be governed primarily by electrostatic interactions and polyelectrolyte complexation mechanisms. DNA contains highly negatively charged phosphate groups (PO_4^{2-}) along its backbone, which can interact with protonated amine groups introduced into the modified

SMA copolymer. These interactions lead to charge neutralization and charge screening, reducing electrostatic repulsion between DNA strands and promoting DNA condensation into compact structures. This type of interaction is commonly observed in systems involving cationic polymers and nucleic acids, where the formation of polymer–DNA complexes is driven by electrostatic attraction and counterion release (Kabanov & Zezin, 1984; Bloomfield, 1997; Mintzer & Simanek, 2009).

As a result, the SMA–DNA mixture forms flocculates enriched in polymer–DNA complexes, which may represent a reversible and controllable process for DNA condensation without severe structural damage to the nucleic acid. In this system, the long hydrophobic chains derived from the tallow amine are not expected to interact directly with the negatively charged DNA backbone. Instead, these hydrophobic segments likely contribute to the stabilization of the polymer–DNA complexes, promoting structural compaction of the assemblies through hydrophobic interactions within the polymer matrix.

Overall, these results suggest that the modified SMA copolymer interacts with biomacromolecules through distinct mechanisms depending on their structural and electrostatic properties: protein aggregation driven by hydrophobic and charge neutralization effects in the case of albumin, and polyelectrolyte complexation leading to DNA condensation in the case of nucleic acids.

Figure 7 illustrates the molecular structures used to visualize the possible interactions between the modified SMA copolymer and a DNA fragment. In Figure 7a, a three-dimensional representation of the

system is presented, where regions with different colors correspond to molecular interaction fields (MIFs), sometimes described as lipophilicity or hydrophobicity interaction maps. These maps are commonly used in molecular modeling to identify potential interaction regions between macromolecules and ligands. The blue spheres correspond to hydrophobic regions. These areas are mainly associated with the aromatic rings of the styrene units and the hydrocarbon chains derived from the tallow amine modifier. The presence of these hydrophobic domains suggests a strong affinity for nonpolar environments and indicates that weak π – π interactions between aromatic rings may contribute to intermolecular association and self-assembly of the copolymer. Such interactions are likely responsible for the formation of the hydrophobic core of the polymer aggregates or micelle-like structures. In addition, green spheres represent regions with intermediate hydrophobicity or amphiphilic character. These areas can interact weakly with both hydrophobic and polar domains, acting as flexible interfaces between hydrophobic and hydrophilic environments. In the present model, these regions are more frequently observed near the DNA segments and may contribute to a flexible coupling between the hydrophobic polymer domains and the polar DNA backbone. Finally, a smaller number of orange spheres can be observed, mainly located near the DNA fragment. These regions correspond to transition zones toward higher polarity, typically located close to polar functional groups. Such sites are capable of forming electrostatic interactions and hydrogen bonds, which are particularly relevant in polymer–DNA complexes where the negatively charged phosphate groups of DNA interact with protonated amine

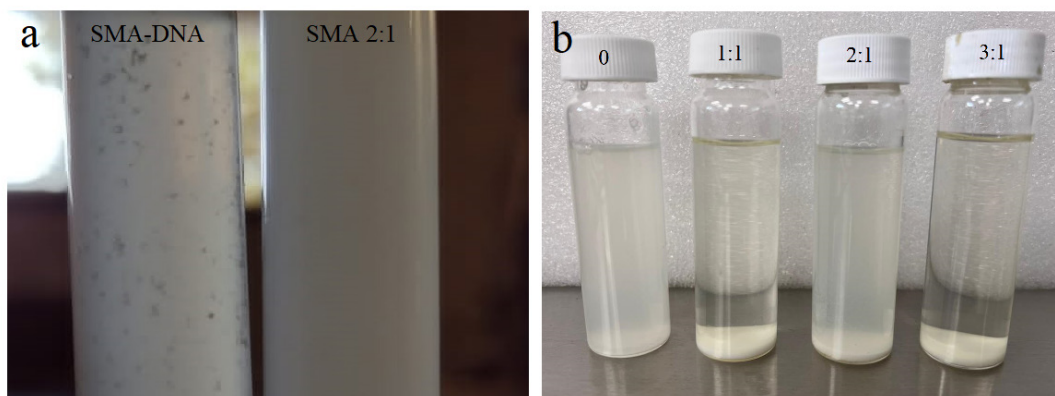


Figure 6. Appearance of condensation of: a) SMA—ADN y a) SMA-egg albumin

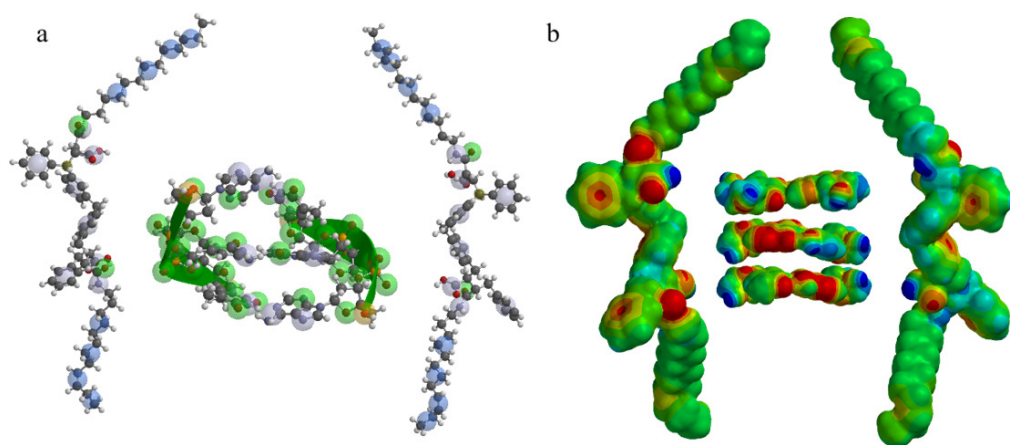


Figure 7. Theoretical calculation of a) CFD map and B) electrostatic potential map of SMA-DNA

groups in the polymer. Figure 7b shows the electrostatic potential surface calculated for a segment of the modified SMA copolymer together with fragments representing amino acid residues (arginine and cysteine) and a nucleobase (thymine). In this representation, red regions indicate electron-rich and negatively charged domains, typically associated with highly hydrophilic functional groups. In contrast, blue regions correspond to electron-deficient or positively charged sites, which are responsible for electrostatic interactions with negatively charged species such as the phosphate groups present in the DNA backbone. The green regions represent electrostatically neutral domains, which do not directly participate in electrostatic attraction but contribute to the structural stability of the assemblies by promoting hydrophobic packing and facilitating the self-assembly of micelle-like structures that surround the complex and protect it from the aqueous environment.

This type of computational analysis is widely used to evaluate molecular compatibility, intermolecular interactions, and potential binding regions in polymer–biomolecule systems, providing valuable insight into the mechanisms of supramolecular assembly and biomolecular recognition. [Vargas 2025, Turker 2024, Reyes 2019]

Conclusions

In this work, it was demonstrated that styrene–maleic acid (SMA) modified with tallow amines acts as an effective amphiphilic platform capable of interacting in a differentiated manner with biomolecules of distinct nature. The system exhibited a clear ability to condense DNA through predominantly electrostatic interactions, while indu-

cing the precipitation of egg albumin via a mechanism associated with charge neutralization and the strengthening of hydrophobic interactions.

FTIR characterization, together with spectral subtraction analysis, revealed spectral contributions associated with phosphate groups and nitrogenous base residues (guanine, cytosine, among others). These observations confirm the participation of non-covalent interactions in the formation of the SMA–biomolecule complexes. Optical micrographs further revealed the formation of condensed and encapsulated structures in the case of DNA, showing compact domains consistent with flocculation and controlled self-assembly processes.

Additionally, theoretical calculations based on molecular interaction fields (MIFs) and electrostatic potential maps indicated a clear charge complementarity between the protonated amine groups of the modified SMA and the negatively charged DNA backbone. These results support the electrostatic and potentially reversible nature of the DNA condensation process.

Overall, these findings demonstrate that hydrolyzed SMA functionalized with tallow amines can discriminate between different biomolecules, promoting reversible DNA condensation and controlled protein precipitation. This behavior opens new opportunities for the development of functional materials, including systems for biomolecule encapsulation, emulsion stabilization, and separation technologies for the environmental remediation of organic contaminants in aqueous media.

References

- Wood, B. R. (2016). The importance of hydration and DNA conformation in interpreting infrared spectra of cells and tissues. *Chemical Society Reviews*, 45(7), 1980-1998.
- Mao, Y., Daniel, L. N., Whittaker, N., & Saffioti, U. (1994). DNA binding to crystalline silica characterized by Fourier-transform infrared spectroscopy. *Environmental Health Perspectives*, 102(suppl 10), 165-171.
- Xiaopin Duan, Jishen Xiao, Qi Yin, Zhiwen Zhang, Shirui Mao, aping Li. Amphiphilic raft copolymer based on poly(styrene-co-maleic anhydride) with low molecular weight polyethyleneimine for efficient gene delivery. *International Journal Nanomedicine*, 2012, 7: 4961-72
- Winel CL, Burgun JJ. Acute and subacute toxicology and safety evaluation of SMA 1440-H resin *Clin toxicology* 1977, 10 (2): 255-260
- Maeda H. SMANCS and polymer-conjugated macromolecular drugs: advantages in cancer chemotherapy. *Adv Drug Deliv Rev*. 2001;46(1-3) 169-185
- Zovko M, Barbaric M, Zorc B, Hafner A, Filipovic-Grcic J. Synthesis of Fenopropfen and gemfibrozil styrene-maleic acid copolymer conjugates. *Acta Pharm*, 2005; 55(2): 169-176
- Klosgen, B.; et al *Biochemistry* 2009 48, 10823-0842
- Knowles, T; et al *Nat. Protoc* .2009 ,4, 1013-1021
- Jamshad, M., Lin, Y. P., Knowles, T. J., Parslow, R. A., Harris, C., Wheatley, M., ... & Dafforn, T. R. (2011). Surfactant-free purification of membrane proteins with intact native membrane environment. *Biochemical Society Transactions*, 39(3), 813-818.
- , J. M., Scheidelaar, S., Koorengel, M. C., Dominguez, J. J., Schäfer, M., van Walree, C. A., & Killian, J. A. (2016). The styrene-maleic acid copolymer: a versatile tool in membrane research. *European Biophysics Journal*, 45(1), 3-21.
- Oluwole, A. O., Danielczak, B., Meister, A., Babalola, J. O., Vargas, C., & Keller, S. (2017). Solubilization of membrane proteins into functional lipid-bilayer nanodiscs using a diisobutylene/maleic acid copolymer. *Angewandte Chemie International Edition*, 56(7), 1919-1924.
- Godbey, W. T., Wu, K. K., & Mikos, A. G. (1999). Size matters: molecular weight affects the efficiency of poly (ethyleneimine) as a gene delivery vehicle. *Journal of Biomedical Materials Research: An Official Journal of The Society for Biomaterials, The Japanese Society for Biomaterials, and The Australian Society for Biomaterials*, 45(3), 268-275.
- Marc Lavertu, Stephane Méthot, Nicolas Tran-Khanh, Michael D. Buschmann, High efficiency gene transfer using chitosan/DNA nanoparticles with specific combinations of molecular weight and degree of deacetylation, *Biomaterials*, Volume 27, Issue 27, 2006, Pages 4815-4824, <https://doi.org/10.1016/j.biomaterials.2006.04.029>.
- Mintzer, M.A.; Simanek, E.E. *Chem Rev*, 2009, 109, 29-302
- Lynn, D. M., & Langer, R. (2000). Degradable poly (β -amino esters): synthesis, characterization, and self-assembly with plasmid DNA. *Journal of the American Chemical Society*, 122(44), 10761-10768.
- Felgner, P. L., Gadek, T. R., Holm, M., Roman, R., Chan, H. W., Wenz, M., ... & Danielson, M. (1987). Lipofection: a highly efficient, lipid-mediated DNA-transfection procedure. *Proceedings of the National Academy of Sciences*, 84(21), 7413-7417.

Wagner, E., Curiel, D., & Cotten, M. (1994). Delivery of drugs, proteins and genes into cells using transferrin as a ligand for receptor-mediated endocytosis. *Advanced Drug Delivery Reviews*, 14(1), 113-135.

Kabanov, A. V., & Kabanov, V. A. (1995). DNA complexes with polycations for the delivery of genetic material into cells. *Bioconjugate chemistry*, 6(1), 7-20.

Harding, J., et al. (2019) Effect of styrene-maleic acid copolymer composition on nanodisc formation. *Langmuir*.

Ravula, T., **Hardin, N. Z.**, & Ramamoorthy, A. (2019). Polymer nanodiscs: Advantages and limitations. *Chemistry and physics of lipids*, 219, 45-49.

Vargas-Rubio K.I.; Delgado E.;Cabrales-Arellano C.P.;Gamboa-Gomez C.I.; & Reyes-Jaquez D. 2025. Computational Modeling Approaches for optimizing microencapsulation Processes: from molecular dynamics to CFD and FEM techniques. *BioPhysica*(4) 49.

Turker L. Effect of perturbation on dantrolene-A DFT treatise. *Earthline Journal of chemical science* 11(3), 457-470

N B D Reyes and B B Pajarito 2019 Computational design of dummy molecularly imprinted polymers via hydrogen bonding investigation for oxytetracycline determination *IOP Conf. Ser.: Mater. Sci. Eng.* **634** 012035

Tang, C., Ye, S., & Liu, H. (2007). Electrosspining of poly (styrene-co.malic anhydride) (SMA) and water swelling behavior of Cross-linked/Hydrolyzed SMA hydrogel nanofibers. *Polymer*, 48(15), 4482-4491.

Wang, M., Zhu, X., & Zhang, L., (2000). Hole structure and its formation in thin films of hydrolyzed poly(Styrene maleic anhydride) alternating copolymers. *Journal of applied polymer science*, 75(2), 267-274

Muntean,, C.M., Lapusan, A., Mihaiu, L. & Stefan, ,R. Strain Dependent UV degradation of *Scheriquia coli* DNA monitored by Fourier Transform infrared spectroscopy, ,J. Photochem. Photobiol, B Biol. 130. 140-145(2014)

Pevsner, A. & Diem, M. infrared spectroscopic studies of major cellular components, Part II: The effect of hydration on the spectra of nucleic acids. *Appl. Spectrosc.* 55 1502-1505 (2001).

Custovic, I., Pocholle, N., Bourillot, E., Lesnieska, E., & Piétrement. O., (2022). Infrared spectroscopic imaging of DNA molecules on mica surface. *Scientific Reports*, 12(1), 18972

Craig, A. F., Clark, E. E., Sahu, I. D., Zhang, R., Frantz, N. D., Al-Abdul-Wahid, M. S., ... & Lorigan, G. A. (2016). Tuning the size of styrene-maleic acid copolymer-lipid nanoparticles (SMALPs) using RAFT polymerization for biophysical studies. *Biochimica et Biophysica Acta (BBA)-Biomembranes*, 1858(11), 2931-2939.

Harding, B. D., Dixit, G., BurrIDGE, K. M., Sahu, I. D., Dabney-Smith, C., Edelmann, R., ... & Lorigan, G. A. (2019). Characterizing the structure of styrene-maleic acid copolymer-lipid nanoparticles (SMALPs) using RAFT polymerization for membrane protein spectroscopic studies. *Biophysical Journal*, 116(3), 517a.

Lee, J., Bae, J., Kim, W., & Lee, S. (2022). A study on aqueous dispersing of carbon black nanoparticles surface-coated with styrene maleic acid (SMA) copolymer. *Polymers*, 14(24), 5455.

Muntean, C. M., Lapusan, A., Mihaiu, L., & Stefan, R. (2014). Strain dependent UV degradation of *Escherichia coli* DNA monitored by Fourier transform infrared spectroscopy. *Journal of Photochemistry and Photobiology B: Biology*, 130, 140-145.

Banyay, M., Sarkar, M., & Gräslund, A. (2003). A library of IR bands of nucleic acids in solution. *Biophysical chemistry*, 104(2), 477-488.

Lee, S.M.; Yeh, W.L.; Wnag, C.C.; Chen, C.Y. the study on the conductivity of sturene-maleic abhidride copolymer electrolytes based on poly(ethylene glycol) 400 and LiCLO₄, Journal; Electrochimimica Acta, 2004, 49, 2667-2673

Florjanczyk, Z.; Wodzki, R.; Churikov, A.; Lithium gel polyelectrolyte based on cross-linked maleic anhydride- styrene copolymer. Jppournal; electrochimia Acta 2000, 45, 3563-3571

Vink, H. Studies of electrical transport processes in polyelectrolite solutions. Journal of the chemical society, Faraday transactions, 1989, 85 699-709.

Bloomfield, V. A. (1997). DNA condensation by multivalent cations. *Biopolymers: Original Research on Biomolecules*, 44(3), 269-282.

Zinchenko, A., & Yoshikawa, K. (2015). Compaction of double-stranded DNA by negatively charged proteins and colloids. *Current Opinion in Colloid & Interface Science*, 20(1), 60-65.

Spruijt, E., Sprakel, J., Stuart, M. A. C., & van der Gucht, J. (2010). Interfacial tension between a complex coacervate phase and its co-existing aqueous phase. *Soft Matter*, 6(1), 172-178.

Wright, D. B., Patterson, J. P., Pitto-Barry, A., Cotanda, P., Chassenieux, C., Colombani, O., & O'Reilly, R. K. (2015). Tuning the aggregation behavior of pH-responsive micelles by copolymerization. *Polymer Chemistry*, 6(14), 2761-2768.

Scheidelaar, S., Koorengel, M. C., van Walree, C. A., Dominguez, J. J., Dörr, J. M., & Killian, J. A. (2016). Effect of polymer composition and pH on membrane solubilization by styrene-maleic acid copolymers. *Biophysical journal*, 111(9), 1974-1986.